Developmental Changes in Ovine Myocardial Glucose Transporters and Insulin Signaling Following Hyperthermia-Induced Intrauterine Fetal Growth Restriction

JAMES S. BARRY,[1] MEREDITH L. DAVIDSEN, SEAN W. LIMESAND, HENRY L. GALAN, JACOB E. FRIEDMAN, TIMOTHY R. H. REGNAULT, AND WILLIAM W. HAY, JR.
University of Colorado School of Medicine, Denver, Colorado 80218

Developmental changes in ovine myocardial glucose transporters and insulin signaling following hyperthermia-induced intrauterine fetal growth restriction (IUGR) were the focus of our study. Our objective was to test the hypothesis that the fetal ovine myocardium adapts during an IUGR gestation by increasing glucose transporter protein expression, plasma membrane-bound glucose transporter protein concentrations, and insulin signal transduction protein concentrations. Growth measurements and whole heart tissue were obtained at 55 days gestational age (dGA), 90 dGA, and 135 dGA (term = 145 dGA) in fetuses from control (C) and hyperthermic (HT) pregnant sheep. Additionally, in 135 dGA animals, arterial blood was obtained and Doppler ultrasound was used to determine umbilical artery systolic (S) and diastolic (D) flow velocity waveform profiles to calculate pulsatility (S – D/mean) and resistance (S – D/S) indices. Myocardial Glut-1, Glut-4, insulin signal transduction proteins involved in Glut-4 translocation, and glycogen content were measured. Compared to age-matched controls, HT 90-dGA fetal body weights and HT 135-dGA fetal weights and gross heart weights were lower. Heart weights as a percent of body weights were similar between C and HT sheep at 135 dGA. HT 135-dGA animals had (i) lower fetal arterial plasma glucose and insulin concentrations, (ii) lower arterial blood oxygen content and higher plasma lactate concentrations, (iii) higher myocardial Glut-4 plasma membrane (PM) protein and insulin receptor β protein (IRβ) concentrations, (iv) higher myocardial glycogen content, and (v) higher umbilical artery Doppler pulsatility and resistance indices. The HT ovine fetal myocardium adapts to reduced circulating glucose and insulin concentrations by increasing plasma membrane Glut-4 and IRβ protein concentrations. The increased myocardial Glut-4 PM and IRβ protein concentrations likely contribute to or increase the intracellular delivery of glucose and, together with the increased lactate concentrations, enhance glycogen synthesis, which allows for maintained myocardial growth commensurate with fetal body growth. Exp Biol Med 231:566–575, 2006

Key words: myocardium; glucose transporters; intrauterine fetal growth restriction; insulin; glycogen

Introduction

Many epidemiologic and basic science investigations have found a strong correlation between fetal growth restriction (IUGR) and the later development of adult diseases such as Type II diabetes and cardiovascular disease (1–6). In the adult with Type II diabetes, a hallmark of diabetes is myocardial "insulin resistance" that involves defects in the insulin signaling pathway responsible for the translocation of Glut-4, the primary insulin-sensitive glucose transporter, to the plasma membrane (7, 8). It has been hypothesized that alterations in the fetal environment that produce IUGR may be causal with regard to the later development of adult cardiovascular disease. Moreover, perturbations in the insulin signaling pathway that ultimately limit myocardial Glut-4 translocation, leading to "insulin resistance," could be initiated in the growth-restricted fetus during development.

Insulin stimulates glucose uptake by recruitment of insulin-sensitive glucose transporters from tubulovesicular elements to the sarcolemma in cardiac muscle (9). A cascade of signaling events is required for this process, including initial insulin binding to its receptor, activation of intracellular receptor autophosphorylation and kinase activity, and subsequent phosphorylation of insulin receptor

This work was supported in part by the National Institutes of Health (NIH) grant T32-HD07186 (W.W.H. and J.S.B.); NIH grant RO1 HD41505 (T.R.H.R.); Colorado Clinical Nutrition Research Unit Pilot and Feasibility Study grant NIH 5 P30 DK 48520 (J.S.B.); NIH grant RO1 DK52138 (W.W.H.); NIH grant KO1 067393 (S.W.L.); University of Colorado Center for Nutrition Metabolic Core Laboratory grant NIH P30-DK048520; the Children's Hospital Young Investigator Award (J.S.B.); and NIH grant 1 R01 HL071990-01A1 (H.L.G.).

[1] To whom correspondence should be addressed at Department of Pediatrics, Section of Neonatology, University of Colorado School of Medicine, The Children's Hospital, 1056 East 19th Avenue, Box B070, Denver, CO 80218. E-mail: shara.knight@uchsc.edu

Received November 2, 2005.
Accepted February 2, 2006.

1535-3702/06/2315-0566$15.00

substrates (IRS), mostly IRS-1 and IRS-2 in the cardiomyocyte (10). IRS proteins act as docking proteins for downstream signaling molecules, including the regulatory subunit (p85α) of PI-3 kinase, leading to increased p110 catalytic activity of the PI-3–kinase complex. PI-3–kinase plays an essential role in insulin-stimulated Glut-4 translocation (11). The signaling pathways downstream from PI-3–kinase include protein kinase B (PKB or Akt) (12). PKB/Akt is phosphorylated, leading to Glut-4 vesicle migration to the sarcolemma (13). The role of these proteins in the adaptation of the fetal myocardium to IUGR is unknown.

Most cases of IUGR derive from chronic placental insufficiency that results in decreased fetal plasma concentrations of glucose, insulin, and oxygen and increased concentrations of lactate (14–17). Studies in fetal sheep (18–20)[1] and rats (21) have shown that fetal glucose restriction and hypoglycemia tend to upregulate insulin action and enhance the capacity for glucose uptake and metabolism by fetal cells and tissues; this is particularly true in skeletal muscle. Such studies revealed that adaptive increases in insulin sensitivity and glucose tolerance persisted into the neonatal period, but by adulthood, these same previously IUGR animals developed insulin resistance and glucose intolerance. Similar results have been obtained for humans (22).

Although such adaptations have been observed in skeletal muscle, little information has been obtained in the fetal myocardium despite the later life development of myocardial insulin resistance in adults who were born with IUGR. Furthermore, it has been observed that fetal myocardial growth is maintained in relation to fetal body growth in the presence of decreased fetal plasma concentrations of glucose and insulin (and oxygen) and increased concentrations of lactate during an IUGR gestation (14), indicating a unique adaptation mechanism for survival.

During a gestation complicated by IUGR, it is important to understand the mechanisms that allow the fetal myocardium to adapt to these unusual substrate changes. We chose to study the myocardial glucose transporters and the related adaptations of insulin signal transduction proteins during an IUGR gestation in fetal sheep to help understand how the fetal myocardium adapts to glucose deficiency and lactate excess. Such information will provide a basis for understanding how such *in utero* adaptations might change over the animal's life span and lead to later life metabolic complications, such as adult myocardial insulin resistance (7, 8). To date, there has been no study that defines those mechanisms in glucose transport or insulin signaling that might develop in the myocardium of the IUGR fetus to account for such adaptations.

To better define Glut-1 and Glut-4 ontogeny, we studied control and growth-restricted fetal sheep from three gestational age groups; 55 days gestational age (dGA; full-term, 147 dGA), when the ovine placenta begins maximal growth and fetal nutrient uptake from the placenta develops; 90 dGA, when placental growth in the sheep plateaus or even decreases, while placental nutrient transport capacity increases to accommodate the rapid fetal growth (23); and 135 dGA, when the smaller IUGR placenta progressively limits nutrient and oxygen transfer to the fetus (16) and limits subsequent fetal growth. By studying three discrete periods in gestation, we were able to identify the ontogeny of Glut-1 and Glut-4 myocardial mRNA and protein concentrations during the second half of gestation in fetal sheep. Secondly, in the late gestation fetal myocardium, we investigated the alterations in key proteins of the insulin signaling pathway associated with Glut-4 translocation. The purpose of these studies was to test the hypothesis that the fetal ovine myocardium would adapt during an IUGR gestation by increasing Glut-1 and Glut-4 cell membrane transporter concentration, increasing insulin signal transduction, and increasing myocardial glycogen content.

Materials and Methods

Experimental Animals. This study was approved by the University of Colorado Health Sciences Center Animal Care and Use Committee. Thirty-five time-mated, mixed-breed (Columbia-Rambouillet) pregnant ewes with a singleton fetus were used for this study. Nineteen ewes were placed in a hyperthermic (HT) environmental chamber starting at ~35 dGA (40°C for 12 hrs/day and 35°C for 12 hrs/day) to produce placental insufficiency–induced late gestation fetal growth restriction (17, 24, 25). Ewes were maintained in the HT chamber until the gestational age of study, except for the 135-dGA group, the ewes from which were removed from the HT chamber at 120 dGA and placed in control conditions until the time of study. Sixteen pairs of fed ewes were placed in a control (C) environment (20°C ± 2°C for 24 hrs/day). The lighting regimen, humidity, temperature cycling, maternal core body temperature, and the diet/feeding of alfalfa hay pellets to animals have been previously described (26) .

Experimental Design and Tissue Preparation. Studies at 55 dGA (C, $n = 5$; HT, $n = 5$) and 90 dGA (C, $n = 5$; HT, $n = 5$) consisted of necropsies. Whole fetal and individual organ weights were measured, and fetal whole heart tissue was harvested, snap frozen in liquid nitrogen, and stored at –80°C (27).

Additional studies were performed on the 135-dGA group (C, $n = 6$; IUGR, $n = 9$). Umbilical arterial Doppler ultrasound velocimetry studies were performed on these animals at 125 dGA (ATL Ultramark 9; Advanced Technology Laboratories, Bellevue, WA). We used blood-flow indices of resistance that are commonly used in clinical practice and have been previously described in the ovine hypothermia model of IUGR, as described by Galan *et al.* (28). Briefly, pregnant ewes were examined supine in a

[1]Limesand SW, Hay WW, Jr. Unpublished data.

Table 1. cDNA Construction for Glut-1, Glut-4, and GAPDH

cDNA	Forward primer (5′–3′)	Reverse primer (5′–3′)	Product base pairs	Accession No.
Glut-1	GACAGGGAGGAGCAAGCCAAA	TAGGGTGAAGCCAGGGATGTG	381	U89029
Glut-4	TCCACCAGCATCTTYGAG	CCCTCAGTCAGGCTCATC	351	AY949177
GAPDH	CCCTATAGTGAGTCGTATTA	AATNAACCCTACTAAAGGG	266	U94889

semirecumbent position. Using an ATL 4.0-MHz abdominal transducer and an angle of insonation of less than 30°, pulse-waved umbilical artery Doppler velocimetry was performed using color-flow Doppler guidance. Pulsatility (systolic [S] – diastolic [D]/mean) and resistance (S – D/S) indices were calculated based on Doppler flow velocity waveform profiles with a minimum of three cardiac cycles. It has been shown that ovine fetuses with elevated pulsatility and resistance indices have elevated mean systemic blood pressures (29).

At 128 dGA, the 135-dGA group had surgery performed under conditions described previously (14). Surgery was performed after 24 hrs of fasting and 12 hrs without water. The ewes were sedated on the morning of surgery with buprenorphine (1 mg/kg subcutaneously), and anesthesia was induced with diazepam (0.11 mg/kg intravenous) and ketamine (4.4 mg/kg intravenous). Surgery was performed under isofluorane (1%–3%) inhalation. After laparotomy and hysterotomy, polyvinyl catheters (1.4-mm outside diameter) were placed in the maternal femoral artery and vein, the uterine vein draining the pregnant horn, and the fetal pedal artery, umbilical artery, and vein. All catheters were tunneled subcutaneously through an incision on the ewe's flank and secured in a plastic pouch. Catheters were flushed daily with a heparinized saline solution (500 u heparin per ml saline). Catheter placement was confirmed at necropsy. Buprenorphine analgesia was administered daily to the ewe for 3 days following surgery.

At 135 dGA, blood samples were obtained for fetal arterial plasma glucose and lactate concentrations (Yellow Springs model 2700 Select; Yellow Springs Instrument Co., Yellow Springs, OH) and plasma insulin concentrations (Mercodia sheep insulin enzyme-linked immunosorbent assay [ELISA]; Alpco Diagnostics, Windham, NH; this method has been validated for the determination of sheep insulin levels to a sensitivity of 0.05 ng/ml and in our laboratory, the interassay and intraassay coefficients of variation were 2.13% and 2.65%, respectively). Blood samples for hemoglobin oxygen content, pH, pCO_2, and pO_2 values were drawn into heparinized capillary syringes and analyzed using an ABL 520 blood gas analyzer (Radiometer Medical, Copenhagen, Denmark). A necropsy was then performed to weigh individual fetal organs and to obtain tissue for snap freezing in liquid nitrogen and storage at –80°C. At a later time, frozen whole heart tissue from all three groups (55-, 90-, and 135-dGA groups) was ground in liquid nitrogen for further RNA extraction and protein isolation.

Generation of Ovine-Specific cDNAs. Whole heart total cellular RNA was extracted using Tri-Reagent methodologies (Molecular Research Center, Inc., Cincinnati, OH). Polyadenylated RNA was reverse-transcribed with Superscript II reverse transcriptase (Invitrogen Life Technologies, Carlsbad, CA). Glut-1, Glut-4, and glyceraldehyde-3-phosphate dehydrogenase (GAPDH) cDNA were amplified with a polymerase chain reaction (PCR) using synthetic oligonucleotides (Invitrogen), as previously described (30) (Table 1). PCR products were TA cloned using TOPO PCR II kit and transformed into Top 10 F′ competent *Escherichia coli* (Invitrogen). Plasmids were purified using QIAprep Spin Miniprep Kit (Qiagen, Inc., Valencia, CA). The ovine GAPDH cDNA generation has been previously described (26). Nucleotide sequence verification was performed using Basic Local Alignment Search Tool (BLAST NCBI, Bethesda, MD) for the ovine-specific Glut-1 and Glut-4 cDNA (Genbank accession U89029 and AY949177).

Myocardial Northern Blot Analysis for Glut-1 and Glut-4 mRNA Concentration. Northern blot analysis was performed as described previously (26, 31). Briefly, 20 μg of total cellular RNA was analyzed and blots probed with [α-^{32}P]dCTP radiolabeled Glut-1, Glut-4, or GAPDH cDNA. Following an overnight hybridization at 42°C and washing, membranes were exposed to a phospho-imaging screen at –80°C until sufficient band density was obtained. The phospho-images were analyzed by densitometry using Image Quantification Software (Molecular Dynamics, Amersham Biosciences, Piscataway, NJ). The hybridization band size of Glut-1, Glut-4, and GAPDH was calculated by extrapolation from an 0.4–9.5-kb RNA ladder (Gibco-BRL, Gaithersburg, MD). mRNA concentrations of glucose transporters were normalized to GAPDH mRNA (mean ± standard error of the mean [SEM]). GAPDH mRNA concentration was not significantly different across gestation or between study groups.

Plasma Membrane (PM) Enrichment and Myocardial Glut-1 and Glut-4 Western Immunoblot Analysis. Frozen whole heart tissue was ground with a mortar and pestle and homogenized in buffer containing 0.25 *M* sucrose, 0.5 m*M* EDTA, 50 m*M* HEPES, 3 m*M* dithiothreitol (DTT), 0.2 m*M* phenylmethylsulfonyl (PMSF), aprotinin (2 μg/ml), and leupeptin (5 μg/ml; homogenization buffer). PM-enriched fractions were pre-

pared by sucrose density centrifugation (32–34). Briefly, homogenate was centrifuged at 1200 *g* for 10 mins at 4°C. Supernatant was collected and stored on ice. The remaining pellet was resuspended in homogenization buffer (see above) and centrifuged again at 1200 *g* for 10 mins. The two supernatants were combined, and an aliquot (whole heart protein) was stored at −80°C. The remaining supernatant was centrifuged at 9000 *g* for 15 mins. Resultant supernatants were centrifuged for 20 mins at 25,000 *g*. Supernatants were collected and centrifuged at 100,000 *g* for 90 mins. The pellet (PM protein-enriched fraction) was washed once and resuspended (0.25 *M* sucrose, 50 m*M* HEPES, 100 m*M* KCl, 5 m*M* $MgCl_2$, aprotinin [2 μg/ml], and leupeptin [5 μg/ml]). PM protein concentration and whole heart protein homogenate were determined using a modified Lowry assay (DC-protein assay; Bio-Rad, Hercules, CA). Enrichment of PM preparations was assessed by immunoblots with mouse monoclonal anti-sodium/potassium adenosine triphosphatase alpha-1 (05–369 Upstate, Lake Placid, NY).

Electrophoresis was performed under reduced conditions on 50-μg aliquots of PM protein fractions from 55-dGA, 90-dGA, and 135-dGA animals and whole heart homogenate from 90-dGA and 135-dGA animals using the Nupage system (Invitrogen) on a 10% sodium dodecyl sulfate–Tris-glycine gel. Proteins were transferred to an ECL nitrocellulose membrane (Amersham) using the Invitrogen mini-cell and blot module. After proper blocking, the blot was incubated with Glut-1 antibody at 1:2000 dilution in 1× PBS-T (AB1340; Chemicon, Temecula, CA) or Glut-4 antibody at 1:3000 dilution in 1× PBS-T (AB1346, Chemicon). The blot was washed at room temperature with 1× PBS-T. The blot was incubated with goat anti-rabbit-HRP (SC-2030; Santa Cruz Biotechnology, Santa Cruz, CA) diluted in blocking buffer at 1:10,000. After extensive washing, the blots were visualized by enhanced chemiluminescence. Blots were exposed to Hyperfilm (Amersham). Resulting band intensities were analyzed densitometrically through NIH-Scion Image software. Ponceau S staining was performed to ensure sufficient and even protein transfer across the entire nitrocellulose membrane to avoid technical difficulties in detection. For blots containing plasma membrane protein samples, variation between immunoblots was controlled for by electrophoresis of a standardized pooled sample on every immunoblot to provide an internal standard to normalize samples. The optical density of each protein identified by the respective antiserum was divided by the internal control protein prior to subjecting intensities to statistical analysis to distinguish treatment differences. For immunoblots containing whole heart protein samples, GAPDH (NB300–221; Novus Biologicals, Inc., Littleton, CO) was used at a dilution of 1:1000 in 1× PBS-T as a housekeeping protein for multiple membranes. Apparent molecular weight for Glut-1 and Glut-4 bands was confirmed by comparison with prestained molecular weight markers (Rainbow Marker; Amersham).

Western Immunoblot Analysis of Insulin Receptor β Protein (IRβ) Subunit, IRS-1, IRS-2, Total Akt, Phosphorylated Akt, and p85α Subunit of PI-3 Kinase. Preparations of whole heart homogenate (from 90-dGA and 135-dGA animals), protein quantification, protein gel loading, electrophoresis, and protein transfer to ECL nitrocellulose membranes were performed as described above for Glut-1 and Glut-4 immunoblot analysis. The blots were incubated with the following dilution of primary antibody in 1× PBS-T at 1:500 for IRβ (SC-711, Santa Cruz Biotechnology), at 1:500 for IRS-1 (SC-559, Santa Cruz Biotechnology), at 1:300 for IRS-2 (SC-8299, Santa Cruz Biotechnology), at 1:1000 for p85 subunit of PI-3–kinase (06–496, Upstate), at 1:500 for Akt (SC-7127, Santa Cruz Biotechnology), at 1:200 for phospho-AKT (Cell Signaling Tech Inc., Beverly, MA), and at 1:2000 for GAPDH. Blots were incubated with the appropriate secondary antibody conjugated to HRP diluted in blocking buffer and visualized by enhanced chemiluminescence. Blots were exposed to Hyperfilm (Amersham). Resulting band intensities were analyzed densitometrically through Scion Image software. GAPDH was used as a housekeeping protein for all immunoblots as it was found not to be significantly different across gestation or between study groups.

Myocardial Tissue Glycogen Analysis and Fetal Plasma Insulin Determination. Glycogen concentration was determined in 135-dGA cardiac tissue stored at −80°C, as previously described (35). Briefly, 100 mg of cardiac tissue was pulverized by mortar and pestle and placed in a 15-ml centrifuge tube containing 2 ml of 30% KOH. The tubes were placed in a boiling water bath for 30 mins for digestion. One hundred and fifty milliliters of homogenate was placed on #1 Whatman filter paper. The filter paper containing homogenate was then placed into 66% ethanol with constant stirring for 30 mins. The filter paper was removed and dried in a warm oven. After cutting the filter paper into small pieces, they were placed into a 15-ml centrifuge tube containing 2 ml of 0.2 *M* acetate buffer (pH 4.8, 0.5% glacial acetic acid, 0.12 *M* sodium acetate) and 25 μl amyloglucosidase (A-1602, Sigma Chemical Co., St. Louis, MO). After adequate mixing, the tubes were placed into a shaking water bath at 37°C for 60 mins. Next, 400 μl of sample was analyzed for glucose concentration in triplicate on a Yellow Springs Analyzer and compared to concurrently run standards of glycogen (G-8876, Sigma Chemical). Results are expressed as μ*M* glucose/g wet weight heart tissue.

In 135-dGA fetuses, plasma insulin levels were determined using a Mercodia sheep insulin ELISA (Alpco Diagnostics). This method has been validated for the determination of sheep insulin levels to a sensitivity of 0.05 ng/ml. In our laboratory, the interassay and intraassay coefficients of variation were 2.13% and 2.65%, respectively, for low-concentration control and 9.68% and 8.50%, respectively, for high-concentration controls.

Statistical Analysis. Results are expressed as mean

Table 2. Fetal Growth Measurements; Results Are Expressed as Mean ± SEM[a]

	55-dGA C	55-dGA HT	90-dGA C	90-dGA HT	135-dGA C	135-dGA HT
Fetal weight (g)	29.9 ± 1.6	28.6 ± 2.1	703.4 ± 44.8 a	514.69 ± 48.6 a	3512.3 ± 144.9 b	1749.6 ± 223.1 b
Heart weight (g)	0.28 ± 0.03	0.28 ± 0.02	5.18 ± 0.4	4.65 ± 0.3	29.5 ± 3.2 c	12.9 ± 1.5 c
Heart/fetal weight (%)	0.93 ± 0.1	1.00 ± 0.1	0.73 ± 0.2	0.94 ± 0.1	0.85 ± 0.1	0.76 ± 0.1
Brain weight (g)	1.3 ± 0.1	1.4 ± 0.2	16.11 ± 1.1	13.4 ± 1.5	45.1 ± 0.6 d	38.7 ± 2 d
Brain/fetal weight (%)	4.4 ± 0.3	4.3 ± 0.1	2.29 ± 0.1	2.6 ± 0.3	1.37 ± 0.1 e	2.1 ± 0.2 e
Brain/liver (%)	57.97 ± 3.2	67.06 ± 3.4	36.78 ± 2.2	53.7 ± 10.4	41.8 ± 1.7 f	78.3 ± 6.9 f

[a] Analysis was performed using Student's unpaired two-tailed *t* test to determine differences between treatment groups at each gestational age. Like lowercase letters indicate significant differences. In 90-dGA animals, HT fetal weight was lower than in C animals (a, $P < 0.02$). HT fetal weight and heart weight were lower than C weights at 135 dGA (b, $P < 0.005$; and c, $P < 0.001$). Fetal brain weight was significantly lower at 135 dGA (d, $P < 0.05$), but brain weight as a percent of fetal weight was higher (e, $P < 0.01$). Brain weight as a percent of liver weight was significantly higher in the 135-dGA animals compared to age-matched controls (f, $P < 0.02$).

± SEM. Fetal growth, umbilical arterial velocimetry, and biochemical and hematologic measurements were analyzed using a two-tailed, unpaired Student's *t* test. When comparing multiple gestational age groups under C or HT conditions, a simple two-way analysis of variance (ANOVA) was used to compare treatment differences between gestational age groups and treatment differences between the groupings at a given gestational age. *Post hoc* analysis was performed using Tukey's test for all possible *ad hoc* comparisons. Results were considered significant at $P \leq 0.05$.

Results

Fetal Growth Measurements. Fetal body weights in the HT group were 27% lower at 90 dGA and 49% lower at 135 dGA (Table 2). Gross heart weights were 44% lower in the HT group at 135 dGA, but heart weight as a percent of body weight was similar between 135-dGA C and 135-dGA HT fetuses. Brain weight as a percent of total fetal weight was greater by 52% in the HT fetuses at 135 dGA. Brain weight as a percentage of liver weight was 87% higher in the HT fetuses at 135 dGA. These growth parameters demonstrate the characteristic features of asymmetric fetal growth restriction.

Fetal Umbilical Arterial Velocimetry. Doppler resistance and pulsatility indices in the umbilical artery were significantly higher in the near-term HT fetuses than in the controls (Table 3). These velocimetry changes are characteristic of asymmetric IUGR that include high-resistance placental blood flow and "brain growth sparing."

Fetal Biochemical and Hematologic Concentrations. The plasma arterial glucose and insulin concentrations were 40% and 61% lower, respectively, in 135-dGA HT fetuses (Table 3). Arterial lactate concentrations were over 3-fold higher in the HT fetuses. Fetal arterial oxygen contents were 54% lower in the HT fetuses. Cardiac tissue glycogen contents were 70% higher in the HT myocardium at 135 dGA.

Glut-1 and Glut-4 Northern and Western Immunoblot Analysis. Glut-1 mRNA concentration was not significantly different between study groups at any of the gestational study times, but it was significantly higher in the myocardium at 135 dGA compared with 90 dGA ($P < 0.05$) (Fig. 1). Whole heart Glut-1 protein concentrations were not significantly different between HT and C animals at 90 dGA or 135 dGA. Glut-1 myocardial PM protein concentrations were significantly lower in near-term animals compared with 55-dGA animals ($P < 0.01$). Glut-1 PM protein concentrations were not significantly different between treatment groups at any of the studied gestational ages (Fig. 2).

Glut-4 mRNA concentration in cardiac tissue was greater at 135-dGA compared with 55-dGA animals ($P < 0.05$), but it was not different between treatment groups (Fig. 3). Whole heart Glut-4 concentrations were not

Table 3. 135-dGA Fetal Arterial Substrate Levels, pH, Insulin Levels, Oxygen Levels, and Umbilical Arterial Doppler Ultrasound Indices. Results Are Reported as Means ± SEM

	Control	HT	*P* value
Arterial plasma glucose (mg/dl)	20.5 ± 0.5	12.4 ± 0.9	<0.001
Arterial plasma insulin (uU/ml)	19.5 ± 4.0	7.6 ± 1.5	<0.01
Arterial plasma lactate (m*M*/liter)	2.0 ± 0.4	6.3 ± 1.9	<0.05
Myocardial glycogen (μ*M* glucose/g heart tissue)	22.1 ± 1.5	37.5 ± 5.1	<0.05
Fetal arterial pH	7.35 ± 0.01	7.31 ± 0.03	NS[a]
Fetal arterial PAO_2 (torr)	18.5 ± 1.0	11.9 ± 1.0	<0.001
Fetal arterial SAO_2 (%)	45.1 ± 2.5	20.8 ± 4.6	<0.001
Arterial oxygen content (m*M*/liter)	2.6 ± 0.1	1.2 ± 0.4	<0.01
Umbilical artery resistance index	0.49 ± 0.1	0.76 ± 0.04	<0.001
Umbilical artery pulsatility index	0.51 ± 0.1	1.2 ± 0.1	<0.001

[a] NS, not significant.

different between 90-dGA and 135-dGA animals or between study groups at these ages. Glut-4 PM protein concentrations were detectable in 55-dGA myocardium, but these concentrations were not quantifiable. Glut-4 PM protein concentrations were higher in 135-dGA myocardium compared with 90-dGA myocardium ($P < 0.01$) and were significantly higher in the HT myocardium at 135 dGA compared to control values ($P < 0.006$) (Fig. 4).

Insulin Signaling Protein Western Immunoblot Analysis. Protein concentrations of IRβ were greater in 135-dGA HT myocardium compared with controls ($P < 0.05$) (Fig. 5). However, whole heart Western blot concentrations of IRS-1, IRS-2, total Akt, phosphorylated Akt, and p85 subunit of PI-3 kinase were not different between 90-dGA and 135-dGA fetuses or between the two study groups.

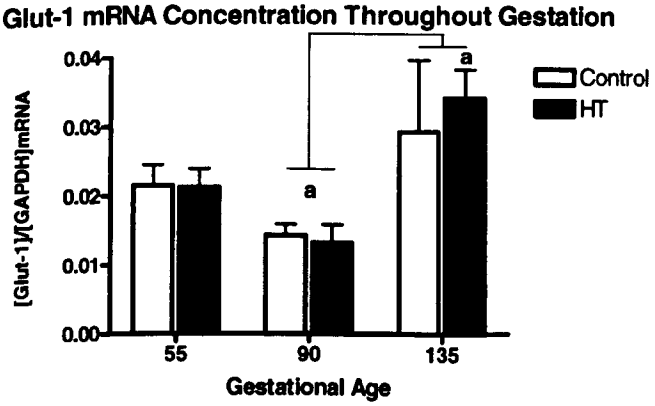

Figure 1. Glut-1 mRNA concentration throughout gestation. Twenty micrograms of total cellular RNA was prepared and probed with ovine-specific Glut-1 cDNA. Glut-1 mRNA concentration (optical density/μg of total cellular RNA) was determined in ovine fetal myocardium at 55 dGA ($n = 10$), 90 dGA ($n = 10$), and 135 dGA ($n = 15$) in C and HT animals by Northern immunoblot analysis. Quantitative densitometric analysis of [Glut-1 mRNA] was expressed per [GAPDH mRNA] (optical density/μg of total cellular RNA) in C and HT myocardium. Data were analyzed using a two-way ANOVA to detect differences across gestation and between study conditions. *Post hoc* analysis was performed using Tukey's test for multiple comparisons. Glut-1 mRNA concentration was higher in 135-dGA myocardium compared with 90-dGA heart tissue (a; $P < 0.05$).

Discussion

The major findings in these studies were that the near-term HT myocardium had higher concentrations of Glut-4 PM protein, higher concentrations of whole heart IRβ protein, and higher glycogen concentrations than did controls. The myocardial weights, relative to fetal weights, were unchanged in the near-term HT animals compared with the controls. Taken together, these observations indicate that the fetal heart exposed to nutrient and oxygen deprivation appears to conserve myocardial energy supply and growth.

This is the first study to report the ontogeny of glucose transporters in the fetal myocardium during the last two-thirds of a normal ovine gestation and in growth-restricted fetal sheep carried by ewes exposed to a HT environment. This environment produces a smaller-than-normal placenta that is associated with a decreased supply of nutrients and oxygen to the fetus relative to fetal weight, resulting in asymmetric fetal growth restriction (17, 36). We also found that the near-term, HT growth-restricted fetuses had higher Doppler velocimetry umbilical artery resistance and pulsatility indices, indicating an increased resistance to placental blood flow.

The predominant cardiac muscle glucose transporters are Glut-1 and Glut-4. Glut-1 is prominent in basal glucose transport, and to a lesser extent may be stimulated by insulin to promote glucose entry into cardiomyocytes (37). Glut-4 is important for insulin-stimulated myocardial glucose uptake (37–39).

Glut-4 plasma membrane concentrations were increased in the IUGR near-term myocardium, whereas plasma membrane concentrations of Glut-1 were unchanged. Studies have determined that Glut-4 has an important role in postnatal cardiac growth, function, and metabolism. Tian and Abel (40) found that Glut-4–deficient hearts developed mild hypertrophy. Belke *et al.* (41) found that cardiac overexpression of Glut-4 resulted in an increase in glucose uptake, increased glycolytic rates, and increased cardiac tissue glycogen concentrations. These two important studies

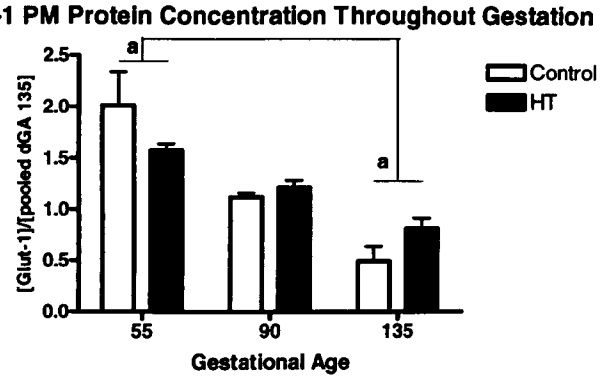

Figure 2. Glut-1 plasma membrane protein concentration throughout gestation. Fifty micrograms of plasma membrane–enriched cardiac tissue protein (PM) from 55-dGA ($n = 10$), 90-dGA ($n = 10$), and 135-dGA ($n = 15$) C and HT animals was probed with Glut-1 antibody. Quantitative densitometric analysis of Glut-1 PM protein concentrations (optical density/μg plasma membrane–enriched cardiac tissue protein) were expressed per [pooled 135-dGA PM] (optical density/μg plasma membrane–enriched cardiac tissue protein), which served as an internal control on multiple blots. Data were analyzed using a two-way ANOVA to detect differences across gestation and between study conditions. *Post hoc* analysis was performed using Tukey's test for multiple comparisons. There were significantly lower Glut-1 PM protein concentrations in 135 dGA compared with 55-dGA myocardium (a; 55 dGA vs. 135 dGA, $P < 0.01$).

illustrate a crucial role of Glut-4 in postnatal myocardial physiology and metabolism in mice. The increase in Glut-4 plasma membrane concentrations in the present studies, therefore, might act in a manner similar to those in postnatal studies to increase or maintain intracellular glucose delivery, glycolytic rates, and cardiac tissue glycogen content.

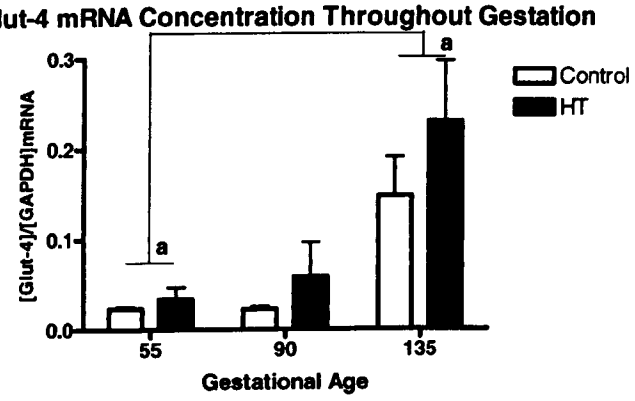

Figure 3. Glut-4 mRNA concentration throughout gestation. Twenty micrograms of total cellular RNA was prepared and probed with ovine-specific Glut-4 cDNA. Glut-4 mRNA concentration (optical density/μg of total cellular RNA) was determined in ovine fetal myocardium at 55 dGA ($n = 10$), 90 dGA ($n = 10$), and 135 dGA ($n = 15$) in C and HT animals by Northern immunoblot analysis. Quantitative densitometric analysis of [Glut-4 mRNA] was expressed per [GAPDH mRNA] (optical density/μg of total cellular RNA) in C and HT myocardium. Data were analyzed using a two-way ANOVA to detect differences across gestation and between study conditions. *Post hoc* analysis was performed using Tukey's test for multiple comparisons. There were significantly higher Glut-4 mRNA concentrations in 135-dGA myocardium compared to 55-dGA myocardial tissue (a; dGA 55 vs. dGA 135, $P < 0.05$).

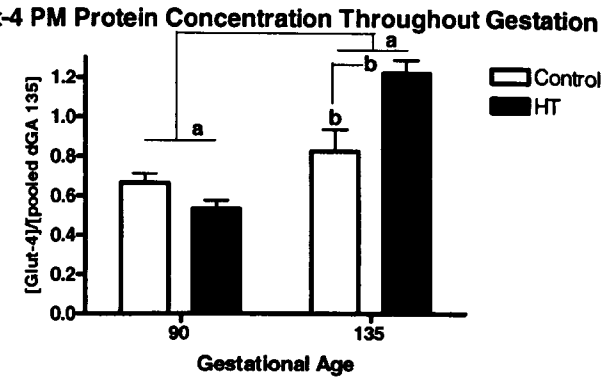

Figure 4. Glut-4 plasma membrane protein concentration throughout gestation. Fifty micrograms of plasma membrane–enriched cardiac tissue protein (PM) from 55-dGA ($n = 10$), 90-dGA ($n = 10$), and 135-dGA ($n = 15$) C and HT animals was probed with Glut-4 antibody. Quantitative densitometric analysis of Glut-4 PM protein concentrations (optical density/μg plasma membrane–enriched cardiac tissue protein) was expressed per [pooled 135-dGA PM] (optical density/μg plasma membrane–enriched cardiac tissue protein), which served as an internal control on multiple blots. Data were analyzed using a two-way ANOVA to detect differences across gestation and between study conditions. *Post hoc* analysis was performed using Tukey's test for multiple comparisons. Glut-4 PM protein concentrations were detectable in 55-dGA myocardium, but were not quantifiable. Glut-4 PM protein concentrations were higher in 135-dGA myocardium compared to 90-dGA myocardium (a; $P < 0.01$). There were significantly higher Glut-4 PM protein concentrations in HT myocardium compared to C at 135 dGA (b; $P < 0.006$).

Mechanisms that might account for the higher myocardial Glut-4 plasma membrane concentrations in the near-term HT animals include myocardial hypoxia, increased cardiac contractility, increased cortisol levels, or increased insulin signal transduction by the increased insulin receptor protein concentrations. While it also is possible that direct effects of hyperthermia on fetal myocardial development and metabolism could have been involved, this is less likely, as other,

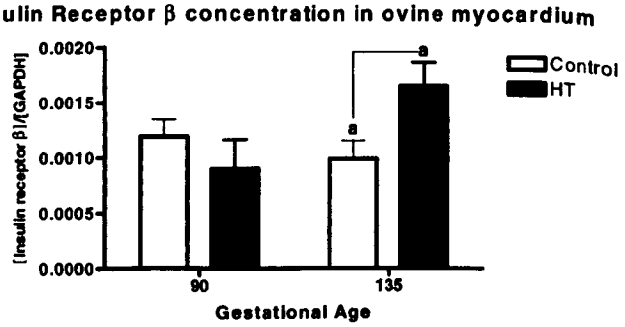

Figure 5. Insulin receptor β protein concentration. Fifty micrograms of whole heart homogenate protein from 90-dGA ($n = 10$) and 135-dGA ($n = 15$) C and HT animals was probed with insulin receptor β antibody. Quantitative densitometric analysis of insulin receptor β concentrations (optical density/μg whole heart homogenate protein) were expressed per GAPDH protein concentrations (optical density/μg whole heart homogenate protein). Data were analyzed using a two-way ANOVA to detect differences across gestation and between study conditions. *Post hoc* analysis was performed using Tukey's test for multiple comparisons. Significantly higher concentrations of the insulin receptor β protein were found in the HT myocardium in 135-dGA animals than in C animals (a; $P < 0.05$).

very different models of ovine fetal IUGR from placental insufficiency and nutrient restriction (adolescent pregnant ewe model [42, 43] and uterine caruncleclectomy model [44]) have similar late gestation phenotypes with respect to increased fetal glucose and insulin sensitivity, despite low circulating fetal glucose and insulin concentrations. Furthermore, while *in vitro* studies (45) have demonstrated increased translocation of Glut-4 in response to acute hyperthermia with no evidence of permanence of this effect, if such effects were pronounced in this hyperthermia model of fetal growth restriction, they should have been seen at 55 and 90 dGA, which they were not. It also is likely that they would have disappeared at 135 dGA, when the animals were studied, because the studies were done 15 days after they were removed from the HT environmental chambers. Thus, although hyperthermia itself cannot be excluded as a mechanism for the observed increased Glut-4 translocation with the current study design, it is not a likely mechanism responsible for the observed changes in late gestation.

Hypoxia and increased cardiac contractility induce Glut-4 translocation to the cell membrane in the cardiomyocyte independent from insulin receptor activation (46–48). Studies of adult cardiomyocyte hypoxia have shown increased Glut-1 and Glut-4 concentrations (49). In the current studies, however, only Glut-4 concentrations were increased, while Glut-1 concentrations were unchanged; these results are consistent with results obtained in the left ventricle (but not the right ventricle) of fetal sheep following 7 days of experimentally produced anemia (~50% reduction in blood oxygen content) (50). In cardiac muscle, Glut-4 translocates to the sarcolemma through mechanisms separate from insulin/insulin receptor interactions in response to contractions *via* a protein that initiates activation of the PI-3–kinase catalytic activity independently of the p85α regulatory subunit (47, 48). Galan *et al.* (29) have shown that increased umbilical arterial pulsatility and resistance indices in the IUGR ovine fetus correlate with significantly higher fetal systemic blood pressures and placental vascular resistance. We speculate that the increase in systemic and umbilical arterial resistance may also lead to a compensatory increase in myocardial contractility, which might increase Glut-4 PM protein concentrations to maintain the intracellular delivery of glucose for energy production. Further study is needed in the IUGR ovine fetus to directly determine cardiac work and the associated changes in glucose metabolism.

Some preliminary evidence indicates that translocation of Glut-4 to the plasma membranes in skeletal muscle might increase in response to cortisol, which increases normally in fetal sheep in the last 2 weeks of gestation (51). Fetal cortisol concentrations increase in some rodent models of IUGR (52) and in conditions that produce fetal stress, such as severe hypoxemia (53), that are encountered to variable degrees in IUGR fetuses. Experimental and naturally occurring suboptimal intrauterine conditions, including IUGR, increase hypothalamic-pituitary-adrenal activity and cortisol concentrations (54). In the current study, however, fetal plasma cortisol concentrations were not different between the control and IUGR groups, and within this model of hyperthermia-induced IUGR, cortisol concentrations only appear to increase in male fetuses and those that also have more severe degrees of fetal hypoxemia and increased lactate concentrations (43).

In the present study, the smaller myocardial size in the HT IUGR fetuses was proportional to their lower overall weight. In contrast, the brain-to-body weight ratio was greater by 47% in the HT IUGR fetuses at 135 dGA, illustrating the "brain growth-sparing" characteristic of asymmetrical IUGR. Myocardial growth is accomplished by a complex interaction of various factors, such as hormones (mainly of the insulin/IGF system), substrate delivery, substrate transporters, and cardiac work (55–61). In this model of IUGR, the fetal myocardium must adapt to decreased circulating nutrient and insulin levels to sustain its rates of metabolism and growth.

Two important determinants of myocardial growth were lower in the IUGR fetus in the present study: arterial insulin and glucose concentrations. Other investigations have shown that fetal insulin and insulin-like growth factor concentrations directly correlate with fetal nutrition during gestation (62, 63). The near-term IUGR myocardium in the present studies might indicate adaptation to the lower concentrations of insulin and glucose by increasing the concentrations of the insulin receptor and Glut-4 PM proteins. Insulin receptors are critical in myocardial growth, as studies in postnatal mice with a cardiomyocyte-selective insulin receptor knockout (CIRKO) have demonstrated a crucial role for insulin and insulin receptor interactions in myocardial growth and development. The CIRKO mice had a 22% and a 28% reduction in heart weights and heart weights to body weights ratios, respectively (56). Akt mediates myocardial growth during development and in response to nutrient restriction (64, 65). In these current studies, myocardial protein concentrations of Akt and phosphorylated Akt were unchanged in the late-gestation HT fetus. Therefore, the greater insulin receptor concentrations and maintained concentrations of Akt and phosphorylated Akt found in the near-term ovine IUGR myocardium might represent mechanisms to conserve growth stimulated by insulin through the insulin receptor *via* downstream signaling through Akt. Future studies will be necessary to assess the insulin-regulated mechanisms in the cardiomyocyte that control the rate of amino acid synthesis into protein, cell turnover, and, thus, myocardial growth.

The myocardium of the near-term IUGR ovine fetuses had higher glycogen content than did controls. Fetal myocardial glycogen deposition and metabolism are poorly understood, especially with fetal growth restriction. Myocardial glycogen concentrations vary greatly among animal species during fetal life (66, 67). The myocardium can increase glycogen content independently of increased cardiomyocyte glucose uptake if alternative energy sources

are available. In this model of fetal growth restriction, circulating arterial concentrations of insulin and glucose are lower, while those of lactate, another prominent myocardial substrate, are higher. Cardiac lactate uptake and metabolism are directly related to plasma lactate concentrations (68). It is possible, therefore, that the fetal IUGR myocardium transports glucose intracellularly to undergo glycolysis and glycogen synthesis, while lactate is preferentially oxidized for energy production. This scenario is supported by the study of Goodwin *et al.* (69), which has shown that glucose metabolic products, which undergo oxidation within the myocardium, preferentially come from the breakdown of glycogen instead of extracellular glucose. Furthermore, the myocardium responds to fasting differently than do other tissues. The adult myocardium increases glycogen content with fasting, unlike other organs, such as skeletal muscle and the liver, in which glycogen levels decrease under fasting conditions (70).

In summary, the current study allows insight into the changes in myocardial growth, glucose transporter expression and protein concentrations, and insulin signal transduction protein concentrations during an IUGR gestation with chronic changes of fetal oxygen delivery, substrate availability, hormonal levels, and most likely cardiac work. The IUGR myocardium adapts by increasing glycogen content, Glut-4 PM protein concentrations, and the concentrations of the insulin receptor in the near-term ovine fetus. Currently, *in vivo* studies in the chronically catheterized ovine fetus are being performed to determine myocardial carbohydrate utilization to better understand fetal myocardial metabolic adaptations during an IUGR gestation.

We thank Karen Trembler and David Caprio for their technical support and excellent care of the animals. We would also like to kindly thank Dr. Gary Zerbe for his assistance in statistical analysis.

1. Barker DJ. Early growth and cardiovascular disease. Arch Dis Child 80:305–307, 1999.
2. Barker DJ. Fetal origins of cardiovascular disease. Ann Med 31:3–6, 1999.
3. Barker DJ. In utero programming of cardiovascular disease. Theriogenology 53:555–574, 2000.
4. Godfrey KM, Barker DJ. Fetal nutrition and adult disease. Am J Clin Nutr 71:1344S–1352S, 2000.
5. Gopalakrishnan GS, Gardner DS, Rhind SM, Rae MT, Kyle CE, Brooks AN, Walker RM, Ramsay MM, Keisler DH, Stephenson T, Symonds ME. Programming of adult cardiovascular function after early maternal undernutrition in sheep. Am J Physiol Regul Integr Comp Physiol 287:R12–R20, 2004.
6. Jaquet D, Gaboriau A, Czernichow P, Levy-Marchal C. Insulin resistance early in adulthood in subjects born with intrauterine growth retardation. J Clin Endocrinol Metab 85:1401–1406, 2000.
7. Desrois M, Sidell RJ, Gauguier D, King LM, Radda GK, Clarke K. Initial steps of insulin signaling and glucose transport are defective in the type 2 diabetic rat heart. Cardiovasc Res 61:288–296, 2004.
8. Eckel J, Till M, Uphues I. Cardiac insulin resistance is associated with an impaired recruitment of phosphatidylinositol 3-kinase to GLUT4 vesicles. Int J Obes Relat Metab Disord 24(Suppl 2):S120–S121, 2000.
9. Zorzano A, Sevilla L, Camps M, Becker C, Meyer J, Kammermeier H, Munoz P, Guma A, Testar X, Palacin M, Blasi J, Fischer Y. Regulation of glucose transport, and glucose transporters expression and trafficking in the heart: studies in cardiac myocytes. Am J Cardiol 80:65A–76A, 1997.
10. Kessler A, Uphues I, Ouwens DM, Till M, Eckel J. Diversification of cardiac insulin signaling involves the p85 alpha/beta subunits of phosphatidylinositol 3-kinase. Am J Physiol Endocrinol Metab 280: E65–E74, 2001.
11. Cheatham B, Kahn CR. Insulin action and the insulin signaling network. Endocr Rev 16:117–142, 1995.
12. Burgering BM, Coffer PJ. Protein kinase B (c-Akt) in phosphatidylinositol-3-OH kinase signal transduction. Nature 376:599–602, 1995.
13. Taha C, Klip A. The insulin signaling pathway. J Membr Biol 169:1–12, 1999.
14. de Vrijer B, Regnault TR, Wilkening RB, Meschia G, Battaglia FC. Placental uptake and transport of ACP, a neutral nonmetabolizable amino acid, in an ovine model of fetal growth restriction. Am J Physiol Endocrinol Metab 287:E1114–E1124, 2004.
15. Nicolini U, Hubinont C, Santolaya J, Fisk NM, Rodeck CH. Effects of fetal intravenous glucose challenge in normal and growth retarded fetuses. Horm Metab Res 22:426–430, 1990.
16. Regnault TR, Galan HL, Parker TA, Anthony RV. Placental development in normal and compromised pregnancies—a review. Placenta 23: S119–S129, 2002.
17. Thureen PJ, Trembler KA, Meschia G, Makowski EL, Wilkening RB. Placental glucose transport in heat-induced fetal growth retardation. Am J Physiol 263:R578–R585, 1992.
18. Aldoretta PW, Carver TD, Hay WW Jr. Ovine uteroplacental glucose and oxygen metabolism in relation to chronic changes in maternal and fetal glucose concentrations. Placenta 15:753–764, 1994.
19. Aldoretta PW, Hay WW Jr. Effect of glucose supply on ovine uteroplacental glucose metabolism. Am J Physiol 277(4 Pt 2):R947–R958, 1999.
20. Carver TD, Hay WW Jr. Uteroplacental carbon substrate metabolism and O_2 consumption after long-term hypoglycemia in pregnant sheep. Am J Physiol 269(2 Pt 1):E299–E308, 1995.
21. Hales CN, Desai M, Ozanne SE, Crowther NJ. Fishing in the stream of diabetes: from measuring insulin to the control of fetal organogenesis. Biochem Soc Trans 24:341–350, 1996.
22. Phillips DI, Hirst S, Clark PM, Hales CN, Osmond C. Fetal growth and insulin secretion in adult life. Diabetologia 37:592–596, 1994.
23. Ehrhardt RA, Bell AW. Growth and metabolism of the ovine placenta during mid-gestation. Placenta 16:727–741, 1995.
24. Alexander GWD. Heat stress and development of the conceptus in the domestic sheep. J Agric Sci 76:53–72, 1971.
25. Bell AW, Wilkening RB, Meschia G. Some aspects of placental function in chronically heat-stressed ewes. J Dev Physiol 9:17–29, 1987.
26. Regnault TR, Orbus RJ, Battaglia FC, Wilkening RB, Anthony RV. Altered arterial concentrations of placental hormones during maximal placental growth in a model of placental insufficiency. J Endocrinol 162:433–442, 1999.
27. Mellor DJ, Matheson IC. Daily changes in the curved crown-rump length of individual sheep fetuses during the last 60 days of pregnancy and effects of different levels of maternal nutrition. Q J Exp Physiol Cogn Med Sci 64:119–131, 1979.
28. Galan HL, Hussey MJ, Chung M, Chyu JK, Hobbins JC, Battaglia FC. Doppler velocimetry of growth-restricted fetuses in an ovine model of placental insufficiency. Am J Obstet Gynecol 178:451–456, 1998.
29. Galan HL, Anthony RV, Rigano S, Parker TA, de Vrijer B, Ferrazzi E, Wilkening RB, Regnault TR. Fetal hypertension and abnormal Doppler velocimetry in an ovine model of intrauterine growth restriction. Am J Obstet Gynecol 192:272–279, 2005.
30. Regnault TR, Orbus RJ, de Vrijer B, Davidsen ML, Galan HL, Wilkening RB, Anthony RV. Placental expression of VEGF, PlGF and

their receptors in a model of placental insufficiency-intrauterine growth restriction (PI-IUGR). Placenta 23:132–144, 2002.
31. Kappes SM, Warren WC, Pratt SL, Liang R, Anthony RV. Quantification and cellular localization of ovine placental lactogen messenger ribonucleic acid expression during mid- and late gestation. Endocrinology 131:2829–2838, 1992.
32. Gelardi NL, Rapoza RE, Renzulli JF, Cowett RM. Insulin resistance and glucose transporter expression during the euglycemic hyperinsulinemic clamp in the lamb. Am J Physiol 277(6 Pt 1):E1142–E1149, 1999.
33. Limesand SW, Regnault TR, Hay WW Jr. Characterization of glucose transporter 8 (GLUT8) in the ovine placenta of normal and growth restricted fetuses. Placenta 25:70–77, 2004.
34. Thorens B, Sarkar HK, Kaback HR, Lodish HF. Cloning and functional expression in bacteria of a novel glucose transporter present in liver, intestine, kidney, and beta-pancreatic islet cells. Cell 55:281–290, 1988.
35. Chan TM, Young KM, Hutson NJ, Brumley FT, Exton JH. Hepatic metabolism of genetically diabetic (db/db) mice. I. Carbohydrate metabolism. Am J Physiol 229:1702–1712, 1975.
36. Ross JC, Fennessey PV, Wilkening RB, Battaglia FC, Meschia G. Placental transport and fetal utilization of leucine in a model of fetal growth retardation. Am J Physiol 270(3 Pt 1):E491–E503, 1996.
37. Fischer Y, Thomas J, Sevilla L, Munoz P, Becker C, Holman G, Kozka IJ, Palacin M, Testar X, Kammermeier H, Zorzano A. Insulin-induced recruitment of glucose transporter 4 (GLUT4) and GLUT1 in isolated rat cardiac myocytes. Evidence of the existence of different intracellular GLUT4 vesicle populations. J Biol Chem 272:7085–7092, 1997.
38. Devaskar SU, Mueckler MM. The mammalian glucose transporters. Pediatr Res 31:1–13, 1992.
39. Zorzano A, Sevilla L, Tomas E, Guma A, Palacin M, Fischer Y. GLUT4 trafficking in cardiac and skeletal muscle: isolation and characterization of distinct intracellular GLUT4-containing vesicle populations. Biochem Soc Trans 25:968–974, 1997.
40. Tian R, Abel ED. Responses of GLUT4-deficient hearts to ischemia underscore the importance of glycolysis. Circulation 103:2961–2966, 2001.
41. Belke DD, Larsen TS, Gibbs EM, Severson DL. Glucose metabolism in perfused mouse hearts overexpressing human GLUT-4 glucose transporter. Am J Physiol Endocrinol Metab 280:E420–E427, 2001.
42. Wallace JM, Bourke DA, Aitken RP, Leitch N, Hay WW Jr. Blood flows and nutrient uptakes in growth-restricted pregnancies induced by overnourishing adolescent sheep. Am J Physiol Regul Integr Comp Physiol 282:R1027–R1036, 2002.
43. Wallace JM, Regnault TR, Limesand SW, Hay WW Jr, Anthony RV. Investigating the causes of low birth weight in contrasting ovine paradigms. J Physiol 565(Pt 1):19–26, 2005.
44. Owens JA, Falconer J, Robinson JS. Glucose metabolism in pregnant sheep when placental growth is restricted. Am J Physiol 257(2 Pt 2): R350–R357, 1989.
45. Widnell CC, Baldwin SA, Davies A, Martin S, Pasternak CA. Cellular stress induces a redistribution of the glucose transporter. FASEB J 4: 1634–1637, 1990.
46. Russell RR III, Bergeron R, Shulman GI, Young LH. Translocation of myocardial GLUT-4 and increased glucose uptake through activation of AMPK by AICAR. Am J Physiol 277:t-9, 1999.
47. Till M, Kolter T, Eckel J. Molecular mechanisms of contraction-induced translocation of GLUT4 in isolated cardiomyocytes. Am J Cardiol 80:85A–89A, 1997.
48. Till M, Ouwens DM, Kessler A, Eckel J. Molecular mechanisms of contraction-regulated cardiac glucose transport. Biochem J 346:841–847, 2000.
49. Behrooz A, Ismail-Beigi F. Stimulation of glucose transport by hypoxia: signals and mechanisms. News Physiol Sci 14:105–110, 1999.
50. Ralphe JC, Nau PN, Mascio CE, Segar JL, Scholz TD. Regulation of myocardial glucose transporters GLUT1 and GLUT4 in chronically anemic fetal lambs. Pediatr Res 58:713–718, 2005.
51. Fowden AL, Li J, Forhead AJ. Glucocorticoids and the preparation for life after birth: are there long-term consequences of the life insurance? Proc Nutr Soc 57:113–122, 1998.
52. Ozanne SE, Hales CN. Early programming of glucose-insulin metabolism. Trends Endocrinol Metab 13:368–373, 2002.
53. Challis JR, Sloboda D, Matthews SG, Holloway A, Alfaidy N, Patel FA, Whittle W, Fraser M, Moss TJ, Newnham J. The fetal placental hypothalamic-pituitary-adrenal (HPA) axis, parturition and postnatal health. Mol Cell Endocrinol 185:135–144, 2001.
54. Fowden AL, Giussani DA, Forhead AJ. Endocrine and metabolic programming during intrauterine development. Early Hum Dev 81: 723–734, 2005.
55. Abel ED. Glucose transport in the heart. Front Biosci 9:201–215, 2004.
56. Belke DD, Betuing S, Tuttle MJ, Graveleau C, Young ME, Pham M, Zhang D, Cooksey RC, McClain DA, Litwin SE, Taegtmeyer H, Severson D, Kahn CR, Abel ED. Insulin signaling coordinately regulates cardiac size, metabolism, and contractile protein isoform expression. J Clin Invest 109:629–639, 2002.
57. Cheung CY, Johnson DD, Reyes V. Ontogeny of insulin-like growth factor-I and -II gene expression in ovine fetal heart. J Soc Gynecol Investig 3:309–315, 1996.
58. Deng XF, Rokosh DG, Simpson PC. Autonomous and growth factor-induced hypertrophy in cultured neonatal mouse cardiac myocytes. Comparison with rat. Circ Res 87:781–788, 2000.
59. Lembo G, Hunter JJ, Chien KR. Signaling pathways for cardiac growth and hypertrophy. Recent advances and prospects for growth factor therapy. Ann NY Acad Sci 752:115–127, 1995.
60. Pellieux C, Sauthier T, Aubert JF, Brunner HR, Pedrazzini T. Angiotensin II-induced cardiac hypertrophy is associated with different mitogen-activated protein kinase activation in normotensive and hypertensive mice. J Hypertens 18:1307–1317, 2000.
61. van Kesteren CA, van Heugten HA, Lamers JM, Saxena PR, Schalekamp MA, Danser AH. Angiotensin II-mediated growth and antigrowth effects in cultured neonatal rat cardiac myocytes and fibroblasts. J Mol Cell Cardiol 29:2147–2157, 1997.
62. Gluckman PD, Pinal CS. Regulation of fetal growth by the somatotrophic axis. J Nutr 133(5 Suppl 2):1741S–1746S, 2003.
63. Holt RI. Fetal programming of the growth hormone-insulin-like growth factor axis. Trends Endocrinol Metab 13:392–397, 2002.
64. Shioi T, McMullen JR, Kang PM, Douglas PS, Obata T, Franke TF, Cantley LC, Izumo S. Akt/protein kinase B promotes organ growth in transgenic mice. Mol Cell Biol 22:2799–2809, 2002.
65. Shiojima I, Yefremashvili M, Luo Z, Kureishi Y, Takahashi A, Tao J, Rosenzweig A, Kahn CR, Abel ED, Walsh K. Akt signaling mediates postnatal heart growth in response to insulin and nutritional status. J Biol Chem 277:37670–37677, 2002.
66. Dawes G, Mott J, Shelley H. The importance of cardiac glycogen for the maintenance of life in foetal lambs and newborn animals during anoxia. J Physiol 146:516–538, 1959.
67. Shelley H. Glycogen reserves and their changes at birth. Br Med Bull 17:37–49, 1961.
68. Bartelds B, Knoester H, Beaufort-Krol GC, Smid GB, Takens J, Zijlstra WG, Heymans HS, Kuipers JR. Myocardial lactate metabolism in fetal and newborn lambs. Circulation 99:1892–1897, 1999.
69. Goodwin GW, Ahmad F, Doenst T, Taegtmeyer H. Energy provision from glycogen, glucose, and fatty acids on adrenergic stimulation of isolated working rat hearts. Am J Physiol 274:t-47, 1998.
70. Schneider CA, Nguyen VT, Taegtmeyer H. Feeding and fasting determine postischemic glucose utilization in isolated working rat hearts. Am J Physiol 260:t-8, 1991.